ACS APPLIED MATERIALS & INTERFACES

Research Article

www.acsami.org

Cloth-Based Power Shirt for Wearable Energy Harvesting and Clothes Ornamentation

Suling Li,[†,‡] Qize Zhong,[‡] Junwen Zhong,[‡] Xiaofeng Cheng,[‡] Bo Wang,[‡] Bin Hu,[‡] and Jun Zhou*[,‡]

[†]Institute of Electromechanical and Quality Technology Engineering, Nanning University, Nanning 530200, China

[‡]Wuhan National Laboratory for Optoelectronics, and School of Optical and Electronic Information, Huazhong University of Science and Technology, Wuhan 430074, China

Supporting Information

ABSTRACT: Harvesting ambient mechanical energy from human body motion has attracted great research interest. In this work, a power shirt based on triboelectrification and the electrostatic induction effect between fluorinated ethylene propylene (FEP) and external objects is demonstrated. This power shirt can effectively convert the ambient mechanical energy into electric power, and the working mechanism is systematically discussed. A maximum short-circuit current density of ~0.37 μA/cm^2 and a maximum peak power density of ~4.65 μW/cm^2 were achieved. Simultaneously, 11 blue LEDs were lit by sliding the sleeve and power shirt, indicating the potential application of the power shirt in clothes ornamentation and risk warning. This study develops an efficient path for harvesting human body energy and promoting the development of wearable electronics and smart garments.

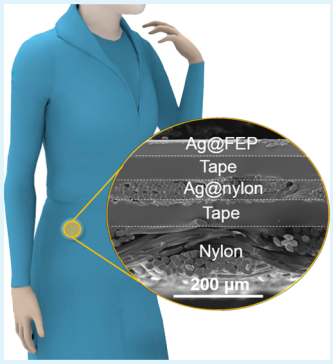

KEYWORDS: *power shirt, triboelectrification, electrostatic induction, clothes ornament, wearable electronics*

INTRODUCTION

Human motion as an energy sources is generally ignored until it is lost to age or death. However, recently, the harvesting of ambient mechanical energy from the surrounding environment has been attracting extensive research efforts, especially from human motions such as limb movements, breathing, and heart beating.[1−4] The collected energy can be supplied for portable or wearable electronics,[5−7] which have seen significant developments in the application fields of human health monitoring, surgery tools, clothes ornaments, and so on, aiming at building self-powered wearable electronic systems. Many advances have been achieved in developing energy-harvesting techniques based on different mechanisms, such as electrostatics,[8,9] piezoelectricity,[10−14] and electromagnetics.[15,16]

The generation of electrostatic charges from mechanical contact and separation is known as the triboelectric effect. Nanogenerators based on the triboelectric effect (TENGs) were recently invented to collect ambient energy or act as self-powered sensors,[17−20] and they have the advantages of high efficiency, low cost, environmental friendliness, and universal availability. Traditional contact-mode and sliding-mode TENGs are composed of two separate components.[21−23] Such structures go against assembling within the human body, limiting the TENGs' applicability for human-body energy harvesting. Consequently, it is highly desirable to develop simple structured and highly efficient new type wearable energy-harvesting devices.

In this work, we designed and fabricated a cloth-based power shirt for harvesting energy from sliding motions such as arm swinging. The working mechanism of the power shirt is based on the change in induced charges between two electrodes due to the change in relative position of two sliding layers.[24,25] Compared to previous sliding-mode TENGs consisting of two components, our power shirt features advantages such as having a simple structure and being cloth-based and skin-friendly. Simultaneously, a maximum short-circuit current density of ~0.37 μA/cm^2 and a maximum peak power density of ~4.65 μW/cm^2 were reached. Furthermore, 11 blue light-emitting diodes (LEDs) arranged as an arrow and fastened on the cloth were lit by sliding of the power shirt with arm-swinging motion, showing the potential application in clothes ornamentation and protecting pedestrians at night.

RESULTS AND DISCUSSION

The detailed fabrication process of the cloth-based power shirt is schematically provided in Figure 1a. First, both a piece of fluorinated ethylene propylene (FEP) film and a piece of nylon cloth were covered with a silver (Ag) electrode on one side by magnetron sputtering to form Ag@FEP and Ag@nylon components. The Ag conductivity performance is illustrated in Figure S1 (Supporting Information) with a relative scanning electron microscopy (SEM) image of the Ag electrode surface, which indicates highly stable performance even when subjected to continuous bending for 24000 cycles. Then, the Ag side of

Received: April 28, 2015
Accepted: June 22, 2015
Published: June 22, 2015

DOI: 10.1021/acsami.5b03680
ACS Appl. Mater. Interfaces 2015, 7, 14912−14916

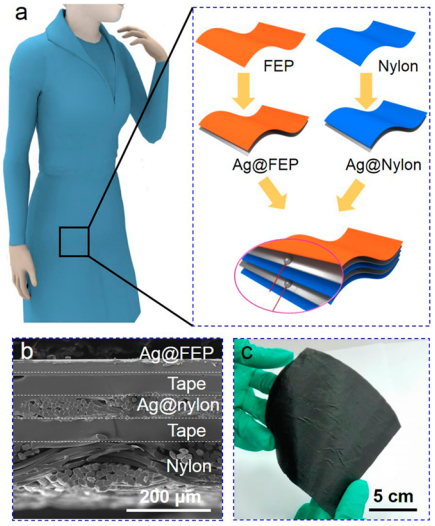

Figure 1. Fabrication of the power shirt. (a) Schematic diagram of the fabrication process of the power shirt. (b) Cross-sectional SEM image of the power shirt. (c) Digital picture of a 10 cm × 10 cm piece of the power shirt.

the Ag@FEP component and the nylon side of the Ag@nylon component were adhered to each other with double-sided adhesive tape, and two conductive wires were drawn out from the two Ag electrodes. Last, a piece of nylon cloth was adhered to the Ag side of the Ag@nylon component as a protective layer. An SEM image of the layer-by-layer structure of the power cloth is provided in Figure 1b, showing that the total thickness is ~300 μm. Figure 1c shows a digital picture of a 10 cm × 10 cm piece of the cloth, demonstrating its excellent flexibility.

The power-generation mechanism of the power shirt is based on triboelectrification and electrostatic induction, as carefully depicted in Figure 2. An external object, such as a piece of nylon cloth, is made to slide with the FEP of the power shirt. In the beginning, triboelectric charges are generated at the contact surfaces, with negative charges $(-Q)$ on the FEP surface and

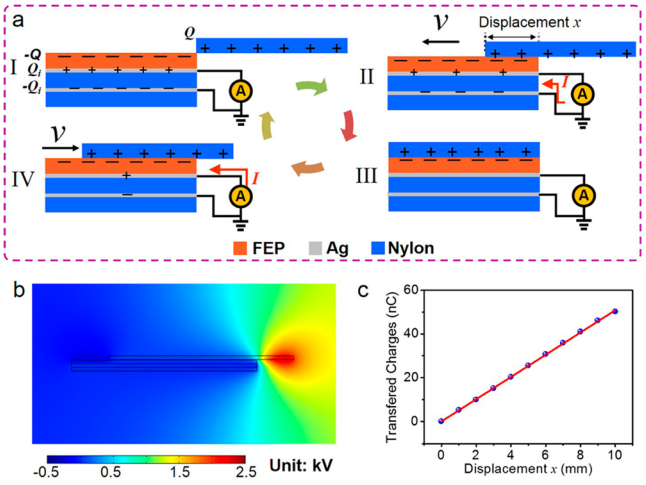

Figure 2. Working mechanism. (a) Schematic diagram illustrating the electricity-generation process in a full cycle, from stage I to stage IV. (b) Potential distribution of a power shirt in the sliding process provided by the COMSOL simulation. (c) Total amount of charge transferred provided by the COMSOL simulation.

positive charges (Q) on the external cloth. By fully sliding the FEP and nylon cloth against each other, both surfaces of the FEP and nylon cloth enter a charge saturated state. After the friction from almost 20 cycles, the surface potential of the FEP reached approximately −350 V and could remain in the saturated state, as shown in Figure S2a,b (Supporting Information). At this point, $Q = |-Q|$.[26,27] The saturated state can remain stable when the power shirt is operated, but once in a nonoperating state, the surface potential of the nylon with positive charges decays rapidly through neutralization with free electrons in the air, as illustrated in Figure S2b (Supporting Information).

The electricity-generation process can be divided into four stages. In stage I, shown in Figure 2aI, two films are fully mismatched, and the charges on the surfaces of both the FEP and nylon enter a saturated state. As a result, the negative charges on the FEP surface cause induced charges on the two Ag electrodes. Positive charges (Q_i) are induced on the top electrode, whereas negative charges $(-Q_i)$ are induced on the bottom electrode, $Q_i = |-Q_i| < |-Q|$.[28−31] Stage I is in equilibrium without charge transfer in the external circuitry. In stage II, the nylon cloth with positive charges starts to slide inward, and Q_i and $-Q_i$ decrease with increasing effective contact area, because of the electrostatic induction of positive charge in the nylon cloth. As a result, induced current flows through top electrode to the bottom electrode to maintain electrostatic equilibrium, as shown in Figure 2aII. When the nylon cloth and FEP reach an overlapping position, the charged surfaces are fully in contact, and both positive charges on the nylon cloth and negative charges on the FEP induce equal but opposite charges on each electrode, reaching an equilibrium state again. The device is then in stage III, which is shown in Figure 2aIII. In stage IV, the nylon cloth starts to slide outward, and then the electrostatic induction of positive charge weakens, causing induced current to flow back from the bottom electrode to the top electrode until electrostatic equilibrium is again reached, as shown in Figure 2aIV.

According to this discussion, the change in relative positions of the two sliding layers leads to a change in the induced charges on the two electrodes, thereby driving the oscillation of the charges between the two electrodes. One can treat such a device as a capacitor,[32−34] with capacitance given by

$$C = \frac{\varepsilon_r \varepsilon_0 S}{d} \tag{1}$$

where ε_0 is the permittivity of a vacuum, ε_r is the relative permittivity of nylon, d is the thickness of nylon cloth between the two electrodes, and S is the surface area of the device. The electric potential between the two electrodes can be expressed as

$$U = \frac{\sigma(S - wx)}{C} = \frac{\sigma(wl - wx)}{C} = \frac{\sigma w}{C}(l - x) \tag{2}$$

Upon substitution of eq 1 into eq 2, we obtain

$$U = \frac{\sigma w}{C}(l - x) = \frac{\sigma w d}{\varepsilon_r \varepsilon_0 S}(l - x) \tag{3}$$

where σ is the negative charge density on the FEP surface, w is the width of the device, l is the length of the device, and x is the displacement of the sliding nylon. Therefore, the transferred charge, ΔQ, can be expressed as

$$\Delta Q = C\Delta U = -\sigma w x \tag{4}$$

DOI: 10.1021/acsami.5b03680
ACS Appl. Mater. Interfaces 2015, 7, 14912−14916

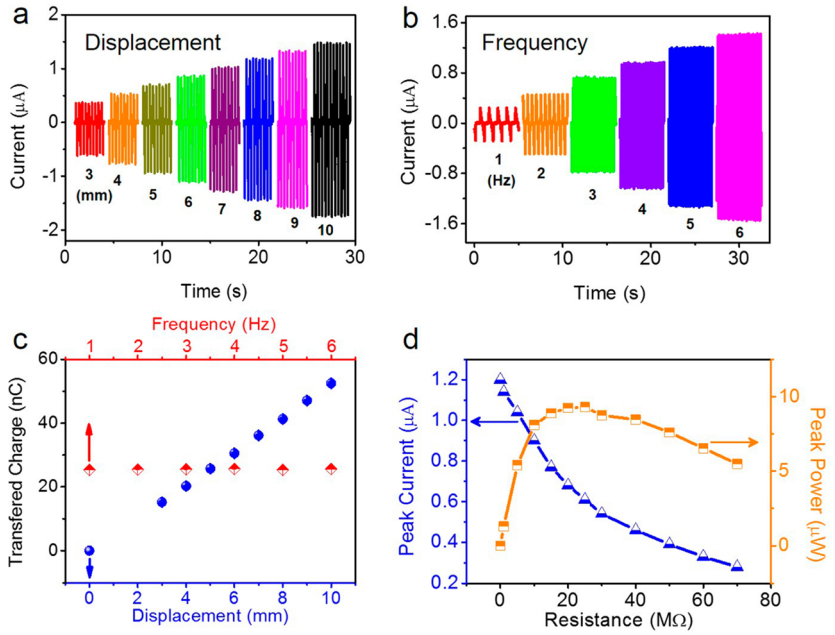

Figure 3. Electrical output performance. Short-circuit currents for the power shirt (a) under a given sliding frequency of 3 Hz with different sliding displacements from 3 to 10 mm and (b) under a given sliding displacement of 5 mm with different sliding frequencies of 1−6 Hz. (c) Total amount of charges transferred under different sliding displacements and different sliding frequencies. (d) Load peak output currents and peak power as functions of the external load resistances at a given sliding frequency of 5 Hz and displacement of 5 mm.

and the external current can, in turn, be expressed as

$$i = \frac{\Delta Q}{\Delta t} = -\sigma w \frac{\mathrm{d}x}{\mathrm{d}t} = -\sigma w v \tag{5}$$

The electric potential distribution and the charge transferred between the two electrodes can be verified through a finite-element simulation based on COMSOL Multiphysics software and the above mathematical derivation. Figure 2b displays the calculated results for the electric potential distribution during the sliding process. As illustrated in Figure 2c, the total amount of charge transferred between the two electrodes increases linearly with the sliding displacement, which can be understood in terms of eq 4.

The output performances of the power shirt were systematically measured. Specifically, a linear motor was utilized to mimic the arm-swinging motion at different frequencies and different displacements during the sliding process, as schematically shown in Figure S3 (Supporting Information).

Based on eq 4, it can be inferred that the output current is directly determined by the sliding displacement and frequency. Figure 3a shows the short-circuit currents of the power shirt with different sliding displacements under a given sliding frequency of 3 Hz. The peak value of the output short-circuit current increased from ∼0.36 to ∼1.48 μA as the sliding displacement was increased from 3 to 10 mm. At the same time, it can be seen in Figure 3b that the peak value of the output short-circuit current increased from ∼0.24 to ∼1.42 μA as the sliding frequency was increased from 1 to 6 Hz for a given sliding displacement of 5 mm, reaching a maximum short-circuit current density of ∼0.37 μA/cm^2.

The values of peak output short-circuit currents are related to both sliding displacement and frequency. However, the total amount of charge transferred is related to only the sliding displacement. The total amount of charge transferred increased linearly from ∼15.7 to ∼52.4 nC when the sliding displacement was increased from 3 to 10 mm, as shown in Figure S4a (Supporting Information) and Figure 3c. This result conforms well with the COMSOL simulation results. On the other hand, the total amount of charge transferred remained constant at ∼25.5 nC under different frequencies ranging from 1 to 6 Hz at a given sliding displacement of 5 mm, as shown in Figure S4b (Supporting Information) and Figure 3c.

Figure 3d displays the load peak current and power as a function of the external load resistance at a given sliding frequency of 5 Hz and displacement of 5 mm. It can be confirmed that, with increasing load resistance, the load peak current decreased step by step. On the other hand, the output power value increased at first and then decreased. The load peak power reached a maximum of ∼9.3 μW when the external resistance was ∼25 MΩ, and a maximum peak power density of ∼4.65 μW/cm^2 was achieved. Additionally, the corresponding open-circuit voltage (V_{oc}) with a maximum value of ∼22 V, tested under the same conditions, is illustrated in Figure S5 (Supporting Information).

As a demonstration of scavenging irregular mechanical energy, such as daily human motions, into electricity to power ornamental electronics for clothes, our power shirt was successfully used as a direct power source without an energy storage system. As shown in Figure 4a, a device with an area of 10 cm × 10 cm was fastened to the shirt below the armpit, which is a location that easily rubs with a sleeve. When the sleeve was sliding with our power shirt, an arrow composed of 11 commercial blue LEDs connected in parallel was instantly illuminated, showing the ornament for the cloth, as indicated in Figure 4b and Video 1 (Supporting Information). Moreover, the light emitted from the LEDs can show the positions of pedestrians on dark nights, ensuring that pedestrians can be seen and avoided by passing cars. When the LEDs were lit, the peak currents went through them is ∼70 μA (Figure 4c). To characterize the washable performance, which is a significant factor to ensure the sustainable usage of an article of clothing, the current performances before and after washing were

DOI: 10.1021/acsami.5b03680
ACS Appl. Mater. Interfaces 2015, 7, 14912−14916

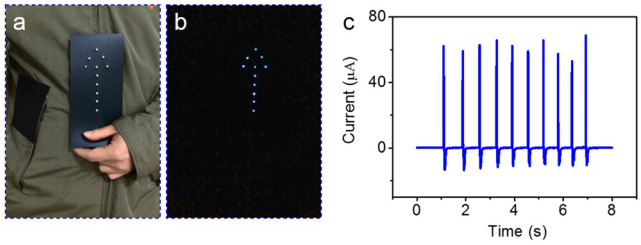

Figure 4. Power shirt for clothes ornamentation and risk warning. Digital pictures of (a) lighting LEDs with the sliding power shirt and sleeve and (b) lit LEDs in the dark. (c) Output current for lighting LEDs.

compared, as shown in Figure S6 (Supporting Information), revealing the outstanding washable performance of the power shirt.

CONCLUSIONS

In conclusion, we have designed and fabricated a simple, lightweight, low-fabrication-cost, and cloth-based power shirt based on triboelectrification between FEP and nylon and the electrostatic induction effect. The detailed working mechanism of the power shirt was carefully explored and discussed. The power shirt had the ability to reach a maximum peak short-circuit current density of ~0.37 μA/cm^2 and a maximum peak power density of ~4.65 μW/cm^2. Furthermore, 11 blue LEDs were lit by sliding the sleeve of the power shirt. Compared to traditional sliding-mode TENGs with two separate components, our power shirt, which integrates both electrodes in one component, exhibits excellent applicability for human-body energy harvesting, which has potential applications in clothes ornamentation and risk warning.

EXPERIMENTAL SECTION

Fabrication of the Cloth-Based Power Shirt. First, both a piece of fluorinated ethylene propylene (FEP) film (4 cm × 4 cm) and a piece of nylon cloth (4 cm × 4 cm) were covered with silver (Ag) electrode on one side by magnetron sputtering to form Ag@FEP and Ag@nylon components. The magnetron sputtering current was 0.15 A, and the sputtering process lasted for 4 min. Then, the Ag side of the Ag@FEP component and the nylon side of the Ag@nylon component were adhered to each other with double-sided adhesive tape, after which two conductive wires were drawn out from the two Ag electrodes. Last, a piece of nylon cloth was adhered to the Ag side of the Ag@nylon component as the protecting layer.

Characterization. The morphology of samples was probed by high-resolution field-emission scanning electron microscopy (FEI Nova NanoSEM 450). The surface potential of FEP was determined with an electrometer (EST102, Huajing, Beijing, China). A linear motor (RCH41 × 30D05A, Renishaw, Gloucestershire, U.K.) was used to carry out the reciprocating friction movements. A piece of nylon cloth was taken as an external object to slide with the power shirt. The electrical output performances of the power shirt was measured with a Stanford low-noise current preamplifier (model SR570).

ASSOCIATED CONTENT

Supporting Information

SEM image of Ag electrode surface; stability test of Ag electrode conductivity; surface potential of the FEP after 0−40 times friction; surface potential decay of nylon and FEP through time after triboelectrification; schematic diagram of the test device setup; output transferred charge as a function of sliding displacement and frequency; open-circuit voltage V_{oc} performance; output current performance comparison before and after washing, and video 1. The Supporting Information is available free of charge on the ACS Publications website at DOI: 10.1021/acsami.5b03680.

AUTHOR INFORMATION

Corresponding Author

*E-mail: jun.zhou@mail.hust.edu.cn.

Notes

The authors declare no competing financial interest.

ACKNOWLEDGMENTS

This work was financially supported by the National Natural Science Foundation of China (51322210, 61434001), the Director Fund of WNLO, and the funds for professor cultivation project of Nanning University (2014JSGC01). The authors acknowledge facility support of the center for Nanoscale Characterization & Devices (CNCD), WNLO-HUST, and the Analysis and Testing Center of Huazhong University of Science and Technology.

REFERENCES

(1) Pu, X.; Li, L.; Song, H.; Du, C.; Zhao, Z.; Jiang, C.; Cao, G.; Hu, W.; Wang, Z. L. A Self-Charging Power Unit by Integration of a Textile Triboelectric Nanogenerator and a Flexible Lithium-Ion Battery for Wearable Electronics. *Adv. Mater.* **2015**, DOI: 10.1002/adma.201500311.

(2) Yang, Y.; Zhang, H.; Zhong, X.; Yi, F.; Yu, R.; Zhang, Y.; Wang, Z. L. Electret Film-Enhanced Triboelectric Nanogenerator Matrix for Self-Powered Instantaneous Tactile Imaging. *ACS Appl. Mater. Interfaces* **2014**, *6*, 3680−3688.

(3) Mitcheson, P. D.; Yeatman, E. M.; Rao, G. K.; Holmes, A. S.; Green, T. C. Energy Harvesting From Human and Machine Motion for Wireless Electronic Devices. *Proc. IEEE* **2008**, *96*, 1457−1486.

(4) Zhong, J.; Zhang, Y.; Zhong, Q.; Hu, Q.; Hu, B.; Wang, Z. L.; Zhou, J. Fiber-Based Generator for Wearable Electronics and Mobile Medication. *ACS Nano* **2014**, *8*, 6273−6280.

(5) Hu, B.; Chen, W.; Zhou, J. High Performance Flexible Sensor Based on Inorganic Nanomaterials. *Sens. Actuators B: Chem.* **2013**, *176*, 552−533.

(6) Zhang, B.; Xiang, Z. M.; Zhu, S. W.; Hu, Q. Y.; Cao, Y. Z.; Zhong, J. W.; Zhong, Q. Z.; Wang, B.; Fang, Y. S.; Hu, B.; Zhou, J.; Wang, Z. L. Dual Functional Transparent Film for Proximity and Pressure Sensing. *Nano Res.* **2014**, *7*, 1488−1496.

(7) Hu, B.; Ding, Y.; Chen, W.; Kulkarni, D.; Shen, Y.; Tsukruk, V. V.; Wang, Z. L. External-Strain Induced Insulating Phase Transition in VO_2 Nanobeam and Its Application as Flexible Strain Sensor. *Adv. Mater.* **2010**, *22*, 5134−5139.

(8) Boland, J.; Chao, Y.; Suzuki, Y.; Tai, Y. C. Micro Electret Power Generator. *Proc. IEEE Annu. Int. Conf. Micro Electro Mech. Syst., 16th* **2003**, 538−541.

(9) Guyomar, D.; Badel, A.; Lefeuvre, E.; Richard, C. Toward Energy Harvesting Using Active Materials and Conversion Improvement by Nonlinear Processing. *IEEE Trans. Ultrason., Ferroelectr., Freq. Control* **2005**, *52*, 584−595.

(10) Nelson, L.; Bowen, C.; Stevens, R.; Cain, M.; Stewart, M. Modelling and Measurement of Piezoelectric Fibers and Interdigitated Electrodes for the Optimisation of Piezofiber Composites. *SPIE Conf. Proc.* **2003**, *5053*, 556−567.

(11) Abdelkefi, A.; Barsallo, N. Comparative Modeling of Low-Frequency Piezomagnetoelastic Energy Harvesters. *J. Intell. Mater. Syst. Struct.* **2014**, *25*, 1771−1785.

(12) Kim, H. S.; Kim, J. H.; Kim, J. A Review of Piezoelectric Energy Harvesting Based on Vibration. *Intl. J. Precis. Eng. Manuf.* **2011**, *12*, 1129−1141.

DOI: 10.1021/acsami.5b03680
ACS Appl. Mater. Interfaces 2015, 7, 14912−14916

(13) Zeng, W.; Tao, X.; Chen, S.; Shang, S.; Chan, H. L. W.; Choy, S. H. Highly Durable All-Fiber Nanogenerator for Mechanical Energy Harvesting. *Energy Environ. Sci.* **2013**, *6*, 2631−2638.
(14) Bai, S.; Zhang, L.; Xu, Q.; Zheng, Y.; Qin, Y.; Wang, Z. L. Two Dimensional Woven Nanogenerator. *Nano Energy* **2013**, *2*, 749−753.
(15) Rome, L. C.; Flynn, L.; Goldman, E. M.; Yoo, T. D. Generating Electricity While Walking with Loads. *Science* **2005**, *309*, 1725−1728.
(16) Donelan, J. M.; Li, Q.; Naing, V.; Hoffer, J. A.; Weber, D. J.; Kuo, A. D. Biomechanical Energy Harvesting: Generating Electricity During Walking with Minimal User Effort. *Science* **2008**, *319*, 807−810.
(17) Zhong, Q.; Zhong, J.; Hu, B.; Hu, Q.; Zhou, J.; Wang, Z. L. A Paper-Based Nanogenerator as a Power Source and Active Sensor. *Energy Environ. Sci.* **2013**, *6*, 1779−1784.
(18) Cottone, F.; Vocca, H.; Gammaitoni, L. Nonlinear Energy Harvesting. *Phys. Rev. Lett.* **2009**, *102*, 080601.
(19) Yang, Y.; Zhang, H.; Lin, Z. H.; Zhou, Y. S.; Jing, Q.; Su, Y.; Yang, J.; Chen, J.; Hu, C.; Wang, Z. L. Human Skin Based Triboelectric Nanogenerators for Harvesting Biomechanical Energy and as Self-Powered Active Tactile Sensor System. *ACS Nano* **2013**, *7*, 9213−9222.
(20) Cheng, X.; Meng, B.; Zhang, X.; Han, M.; Su, Z.; Zhang, H. Wearable Electrode-Free Triboelectric Generator for Harvesting Biomechanical Energy. *Nano Energy* **2015**, *12*, 19−25.
(21) Yang, W.; Chen, J.; Wen, X.; Jing, Q.; Yang, J.; Su, Y.; Zhu, G.; Wu, W.; Wang, Z. L. Triboelectrification Based Motion Sensor for Human−Machine Interfacing. *ACS Appl. Mater. Interfaces* **2014**, *6*, 7479−7484.
(22) Kim, S.; Gupta, M. K.; Lee, K. Y.; Sohn, A.; Kim, T. Y.; Shin, K. S.; Kim, D.; Kim, S. K.; Lee, K. H.; Shin, H. J.; Kim, D. W.; Kim, S. W. Transparent Flexible Graphene Triboelectric Nanogenerators. *Adv. Mater.* **2014**, *26*, 3918−3925.
(23) Cui, N.; Liu, J.; Gu, L.; Bai, S.; Chen, X.; Qin, Y. Wearable Triboelectric Generator for Powering the Portable Electronic Devices. *ACS Appl. Mater. Interfaces* **2014**, DOI: 10.1021/am5071688.
(24) Zhou, T.; Zhang, C.; Han, C. B.; Fan, F. R.; Tang, W.; Wang, Z. L. Woven Structured Triboelectric Nanogenerator for Wearable Devices. *ACS Appl. Mater. Interfaces* **2014**, *6*, 14695−14701.
(25) Zhang, X.; Han, M.; Wang, R.; Zhu, F.; Li, Z.; Wang, W.; Zhang, H. Frequency-Multiplication High-Output Triboelectric Nanogenerator for Sustainably Powering Biomedical Microsystems. *Nano Lett.* **2013**, *13*, 1168−1172.
(26) Niu, S.; Wang, S.; Lin, L.; Liu, Y.; Zhou, Y. S.; Hu, Y.; Wang, Z. L. Theoretical Study of Contact-Mode Triboelectric Nanogenerators as an Effective Power Source. *Energy Environ. Sci.* **2013**, *6*, 3576−3583.
(27) Schaffer, E.; Thurn-Albrecht, T.; Russell, T. P.; Steiner, U. Electrically Induced Structure Formation and Pattern Transfer. *Nature* **2000**, *403*, 874−877.
(28) Bazant, M. Z.; Squires, T. M. Induced-Charge Electrokinetic Phenomena: Theory and Microfluidic Applications. *Phys. Rev. Lett.* **2004**, *92*, 066101.
(29) Lang, N. D.; Kohn, W. Theory of Metal Surfaces: Induced Surface Charge and Image Potential. *Phys. Rev. B* **1973**, *7*, 3541−3550.
(30) Zhang, C.; Tang, W.; Han, C.; Fan, F.; Wang, Z. L. Theoretical Comparison, Equivalent Transformation, and Conjunction Operations of Electromagnetic Induction Generator and Triboelectric Nanogenerator for Harvesting Mechanical Energy. *Adv. Mater.* **2014**, *26*, 3580−3591.
(31) Banerjee, P.; Perez, I.; Henn-Lecordier, L.; Lee, S. B.; Rubloff, G. W. Nanotubular Metal-Insulator-Metal Capacitor Arrays for Energy Storage. *Nat. Nanotechnol.* **2009**, *4*, 292−296.
(32) Seeger, J. I.; Boser, B. E. Charge Control of Parallel-Plate, Electrostatic Actuators and the Tip-in Instability. *J. Microelectromech. Syst.* **2003**, *12*, 656−671.
(33) Beeby, S. P.; Tudor, M. J.; White, N. M. Energy Harvesting Vibration Sources for Microsystems Applications. *Meas. Sci. Technol.* **2006**, *17*, R175−R195.
(34) Zhu, G.; Yang, W. Q.; Zhang, T.; Jing, Q.; Chen, J.; Zhou, Y. S.; Bai, P.; Wang, Z. L. Self-Powered, Ultrasensitive, Flexible Tactile Sensors Based on Contact Electrification. *Nano Lett.* **2014**, *14*, 3208−3213.

DOI: 10.1021/acsami.5b03680
ACS Appl. Mater. Interfaces 2015, 7, 14912−14916